Behavioral/Cognitive

Alzheimer's Disease Pathologies Affect Dopaminergic Neural Mechanisms of Memory

Thomas M. Morin,[1,2] Jordyn L. Cowan,[1] Hsiang-Yu Chen,[1] Jourdan H. Parent,[1,2] Jennifer L. Crawford,[1] Claire J. Ciampa,[1] Vyoma D. Shah,[3] Ming Hsu,[4] William J. Jagust,[3] and Anne S. Berry[1]

[1]Department of Psychology, Brandeis University, Waltham, Massachusetts 02454, [2]A. A. Martinos Center for Biomedical Imaging, Mass. General Hospital Boston, Boston, Massachusetts 02215, [3]Department of Neuroscience, University of California Berkeley, Berkeley, California 94720, and [4]Haas School of Business, University of California Berkeley, Berkeley, California 94720

Aging is accompanied by the disruption of multiple neural systems including alteration in dopamine neurotransmission as well as through the accumulation of neuropathology. Despite broad appreciation that complex mental function relies on integration across systems, there is a general lack of understanding of how multiple age- and disease-related brain features interact to drive variation in performance. To address this gap, we used positron emission tomography in male and female humans to examine independent and combined impacts of dopamine synthesis capacity ([^{18}F]Fluoro-L-*m*-tyrosine) and Alzheimer's disease (AD)-related pathology (amyloid-β: [^{11}C]Pittsburgh Compound B; tau: [^{18}F]Flortaucipir) on memory for rewarding events, which we assessed using functional magnetic resonance imaging ($n = 80$ young and older adults). We specifically probed dopamine synthesis capacity given evidence that it is upregulated in older age and may impart resilience to age-related neural losses. In young adults, higher dopamine synthesis capacity was associated with superior overall memory and greater temporal lobe activation. In older adults, neither dopamine nor AD pathology independently predicted memory performance, though higher dopamine synthesis capacity was associated with memory biases for stimuli associated with rewards rather than losses. Instead, we observed interactions between dopamine synthesis and pathology whereby only older adults with minimal pathology showed preservation of positive dopamine-memory associations. In contrast to resilience accounts, the presence of AD pathology disrupted and even reversed relationships between dopamine synthesis, memory, and temporal lobe activation. These results suggest that AD pathological processes acutely alter the mechanisms by which elevated dopamine synthesis supports optimal memory performance.

Key words: Alzheimer's disease; dopamine; fMRI; memory; PET; reward

Significance Statement

While there is compelling evidence that aging is associated with concomitant alterations in dopamine function and cognition, studies directly linking individual differences in endogenous dopamine with memory performance in older age have shown mixed results. We find that the presence of amyloid-β and tau pathology significantly alters relationships among in vivo measures of dopamine synthesis capacity, brain activity, and behavior such that episodic memory performance appears to be relatively decoupled from the dopamine system in the context of preclinical Alzheimer's disease. These findings suggest that it is critical to account for pathological disease processes when considering the mechanisms by which dopamine influences cognitive function and have implications for understanding the efficacy of therapeutic interventions targeting the dopamine system.

Received Aug. 13, 2025; revised Jan. 12, 2026; accepted Jan. 15, 2026.

Author contributions: M.H., W.J.J., and A.S.B. designed research; V.D.S. and A.S.B. performed research; T.M.M., Jo.L.C., H-Y.C., J.H.P., Je.L.C., V.D.S., and A.S.B. analyzed data; T.M.M., H-Y.C., Je.L.C., C.J.C., M.H., W.J.J., and A.S.B. edited the paper; T.M.M. wrote the paper.

This work was supported by the following grants: National Institutes of Health grants AG058748 (A.S.B.), AG074330 (A.S.B.), AG034570 (W.J.J.), AG062542 (W.J.J.), AG044292 (W.J.J.), AG084259 (T.M.M.), AG089518 (T.M.M.), AG085890 (Je.L.C.), and Alzheimer's Association Award AARF17-530186 (A.S.B.). 3T MR data were collected at the Henry H. Wheeler, Jr Brain Imaging Center, which receives support from the National Science Foundation through their Major Research Instrumentation Program, award number BCS-0821855. Avid radiopharmaceuticals enabled the use of the Flortaucipir tracer but did not provide direct funding and were not involved in data analysis or interpretation. We thank the reviewers for suggesting follow-up analyses that have enhanced this manuscript.

Dr. Morin has served as a consultant for Rocket Science Health. Dr. Jagust has served as a consultant to Biogen, Bioclinica, Roche/Genentech, Eli Lilly, and Grifols and holds an equity interest in OptoCeutics.

Correspondence should be addressed to Anne S. Berry at anneberry@brandeis.edu.

This paper contains supplemental material available at: https://doi.org/10.1523/JNEUROSCI.1580-25.2026

https://doi.org/10.1523/JNEUROSCI.1580-25.2026

Introduction

The mesolimbic dopamine system plays an integral role in reward learning and memory (Murty and Dickerson, 2016). Observations that aging is accompanied by alterations in both dopamine function and cognition have inspired prominent theories that declines in the dopamine system mediate age-related changes in cognition (Bäckman et al., 2006, 2010). Though these theories have found some empirical support (Karalija et al., 2024), other research examining relationships between deficits in dopamine function and poor cognition show mixed results (Juarez et al., 2019; van den Bosch et al., 2023). Moreover, studies of the dopamine system in aging struggle to disentangle dopamine-driven effects from the competing influence of relatively common neuropathological changes on cognition, underscoring the need for a more nuanced consideration of dopamine–cognition relationships in the context of age-related disease.

There are several dopamine-independent alterations in brain function that occur in aging, which may modify relationships between dopamine and cognition. Alzheimer's disease (AD)-related amyloid-β (Aβ) plaques are common in unimpaired individuals, with most studies indicating substantial Aβ accumulation in 30% of adults 70 years and older (Jansen et al., 2015). From studies using tau-PET imaging, there is widespread understanding that medial temporal lobe tau pathology is ubiquitous in aging (Maass et al., 2018). To date the majority of studies examining dopaminergic contributions to cognitive aging have not accounted for AD pathology, which may obscure direct relationships between individual differences in dopamine measures and behavior, particularly for memory performance.

It is also likely that models positing steady and predictable decline in dopamine function across the lifespan are oversimplified. Although there are reductions in dopamine receptor density (Li and Rieckmann, 2014; Karrer et al., 2017), studies suggest that rates of receptor loss are less extreme than previously estimated, are spatially heterogeneous, and show substantial interindividual variability (Rieckmann et al., 2011; Karalija et al., 2024). A growing body of research finds that losses in dopamine receptors may be offset by changes in other components of the system. These complementary changes result in increased synaptic dopamine, via decreased dopamine transporter density (Karrer et al., 2017) and increased activity of dopamine synthesis enzymes, e.g., aromatic amino acid decarboxylase (AADC; Dejesus et al., 2001; Braskie et al., 2008). Recent evidence suggests elevation of dopamine synthesis in aging is compensatory and may, in some cases, provide cognitive resilience to age-related neural losses (Ciampa et al., 2022b). Thus, updated conceptualizations of the dopamine system must recognize the dynamic nature of the system and acknowledge that changes across the lifespan, and relationships with behavior, are non-monotonic.

Accompanying growing appreciation that dopaminergic changes in older age are more complex than previously understood, a complementary literature finds small or inconsistent age effects on some dopamine-dependent cognitive tasks. There is little evidence that healthy aging is associated with systematic deficits in reward anticipation (Samanez-Larkin and Knutson, 2015) or the impact of rewards on incidental learning and subsequent memory (Mather and Schoeke, 2011; Spaniol et al., 2014). More generally, parallel lines of affective research find aging is associated with motivational biases such that there is relative enhancement of memory for positively valenced events and/or dampening of memory for negatively valenced events (Mather and Carstensen, 2005). Developing theoretical frameworks have invoked catecholamine systems as mechanistic drivers of age-related alteration in affective and reward-motivated cognition (Samanez-Larkin and Knutson, 2015; Berry et al., 2019; Mather, 2024). Whether relative preservation or upregulation of some aspects of dopaminergic function underlie the maintenance of reward memory in aging is an open question.

We used PET imaging and task-based fMRI to investigate dopaminergic mechanisms of reward-related memory in youth and aging. Consistent with the extant literature, we found dopamine synthesis capacity was higher in older adults relative to young. Of central interest were analyses characterizing the degree to which elevated dopamine synthesis may bolster memory performance in the face of AD pathological changes or whether those pathological changes fundamentally transform dopamine–cognition relationships observed in youth and normal agers.

Materials and Methods

Participants

Fifty older adults and thirty younger adults were recruited from the ongoing longitudinal Berkeley Aging Cohort Study to participate in the current experiment. Older adults were characterized as cognitively normal using an interview and test battery including subsets of the Wechsler Adult Intelligence Scale-Revised (Wechsler, 1987) and the Mini Mental State Exam (MMSE; Folstein et al., 1975). Older adults scored at least 25 on the MMSE. All participants provided informed consent, and study procedures were approved by the Institutional Review Boards at University of California, Berkeley and Lawrence Berkeley National Laboratory. All participants completed an fMRI scanning session, during which they performed the Real Estate Selling Task (described below). Following the fMRI session, participants completed a surprise memory test for stimuli presented during the scan. Many participants also completed PET imaging scans to measure dopamine synthesis capacity [[^{18}F]Fluoro-L-*m*-tyrosine (FMT)], tau [[^{18}F]Flortaucipir (FTP)], and Aβ [[^{11}C]Pittsburgh Compound-B (PiB)]. Demographic information is presented in Table 1. Detailed information about participant attrition, exclusion, and data collection timelines is presented in Figure S1.

Biomarker groups

Participants were categorized into three biomarker groups: young adults, normal agers, and preclinical AD. The young adults biomarker group consisted of all the young adult participants, who were all healthy and between the ages of 18–35 ($n = 29$). Older adults were assigned into

Table 1. Participant demographics

Measure	Group	*n*	Age M(SD)	% Female	Years Edu. M(SD)
Memory	Younger Adults	29	25.2 (3.67)	41.4%	16.4 (1.70)
	Older Adults	46	76.7 (5.77)	58.7%	16.7 (1.97)
fMRI	Younger Adults	28	25.2 (3.73)	39.3%	16.4 (1.72)
	Older Adults	41	76.5 (5.83)	63.4%	16.7 (2.06)
[^{18}F]FMT PET	Younger Adults	14	25.0 (3.98)	28.6%	15.9 (1.77)
	Older Adults	41	76.7 (5.86)	58.5%	16.6 (2.00)
[^{11}C]PiB PET	PiB- Older Adults (Normal Agers)	30	75.4 (6.21)	56.7%	16.9 (2.07)
	PiB + Older Adults (Preclinical AD)	15	79.1 (4.17)	60.0%	16.5 (1.85)
[^{18}F]Flortaucipir PET	Older Adults	41	76.7 (5.90)	58.5%	16.7 (2.00)

Cognitively normal older and younger adults ($n = 80$) were recruited for this study. All participants completed the Real Estate Selling Task during fMRI. Subsets of participants also completed PET scans to measure dopamine synthesis capacity ([^{18}F]FMT), amyloid load ([^{11}C]PiB), and tau burden ([^{18}F]Flortaucipir). Participant counts (*n*) reflect the final subgroup sizes following quality control procedures.

biomarker groups according to criteria outlined in Jack et al. (2024). The normal agers biomarker group had negative PiB status [$n = 31$; distribution volume ratio (DVR) gray matter/cerebellar gray < 1.065; Villeneuve et al., 2015]. The preclinical AD biomarker group had positive [^{11}C]PiB status (DVR > 1.065) with either a negative tau scan (Braak Stage III/IV regions SUVR < 1.26; Jack Stage A; $n = 9$) or a positive tau scan (Braak Stage III/IV regions SUVR > 1.26; Jack Stage B; $n = 6$; Jack et al., 2024; Landau et al., 2024).

Real Estate Selling Task

During fMRI scanning, participants performed the probabilistic learning phase of the "Real Estate Selling Task" (Fig. 1*A*). Participants were told they owned a portfolio of houses and worked with three real estate agents to sell them. Each agent had a distinctive outcome pattern: one typically sold for a profit (reward agent), one always broke even (neutral agent), and one typically sold at a loss (loss agent). Participants were instructed to learn and label each agent's identity (reward/neutral/loss) based on repeated feedback. Each trial consisted of: (1) cue phase (2.0 s), a real estate agent was shown and participants identified the agent as "reward," "neutral," or "loss" using one of three buttons; (2) delay phase (2.4–4.8 s); (3) target phase (3.0 s), a house image appeared, outlined in green (profit), gray (break-even), or red (loss) to indicate outcome of the sale; (4) feedback phase (1.0 s), monetary outcome displayed, +$1 (reward), −$0.50 (loss), or "=" (neutral); and (5) intertrial interval (2–10 s, jittered). Trial outcomes were predetermined to optimize orthogonality across conditions for event-related fMRI analyses. If a participant failed to respond during the cue phase, then the target phase showed a house overlaid with "?" and a blank screen was displayed during the feedback phase. These nonresponse trials were marked as incorrect. Agent-outcome contingencies were as follows: (1) reward agent, 80% profit, 20% loss; (2) loss agent, 80% loss, 20% profit; (3) neutral agent, 100% break-even. Participants were not informed of these probabilities and were told to categorize agents based on their typical outcomes, not to predict individual trials. Participants completed four runs of the task (42 trials each; 168 total trails). In the first two runs, all realtors were of the same gender (male or female), and to counterbalance the final two runs showed realtors all from the opposite gender. There were 56 unique realtor-house pairings (28 male, 28 female); each pairing was presented three times across all runs.

Quantification of memory ability

Memory for the house images was assessed ~30 min after MRI scanning. Participants saw 72 house images and indicated whether they had previously seen each image: "Yes," "Likely Yes," "Likely No," or "No" (Fig. 1*B*). Of the stimuli shown, 16 were lure images of houses that they had never seen before, and 56 were images of the houses previously displayed during the probabilistic learning phase (16 reward, 16 neutral, 16 loss, and 8 "surprise trials" that were unexpectedly sold at a profit/loss by the reward/loss realtor). Analyses focused on high-confidence memory trials rated "Yes/No." Surprise trials were omitted from all memory analyses.

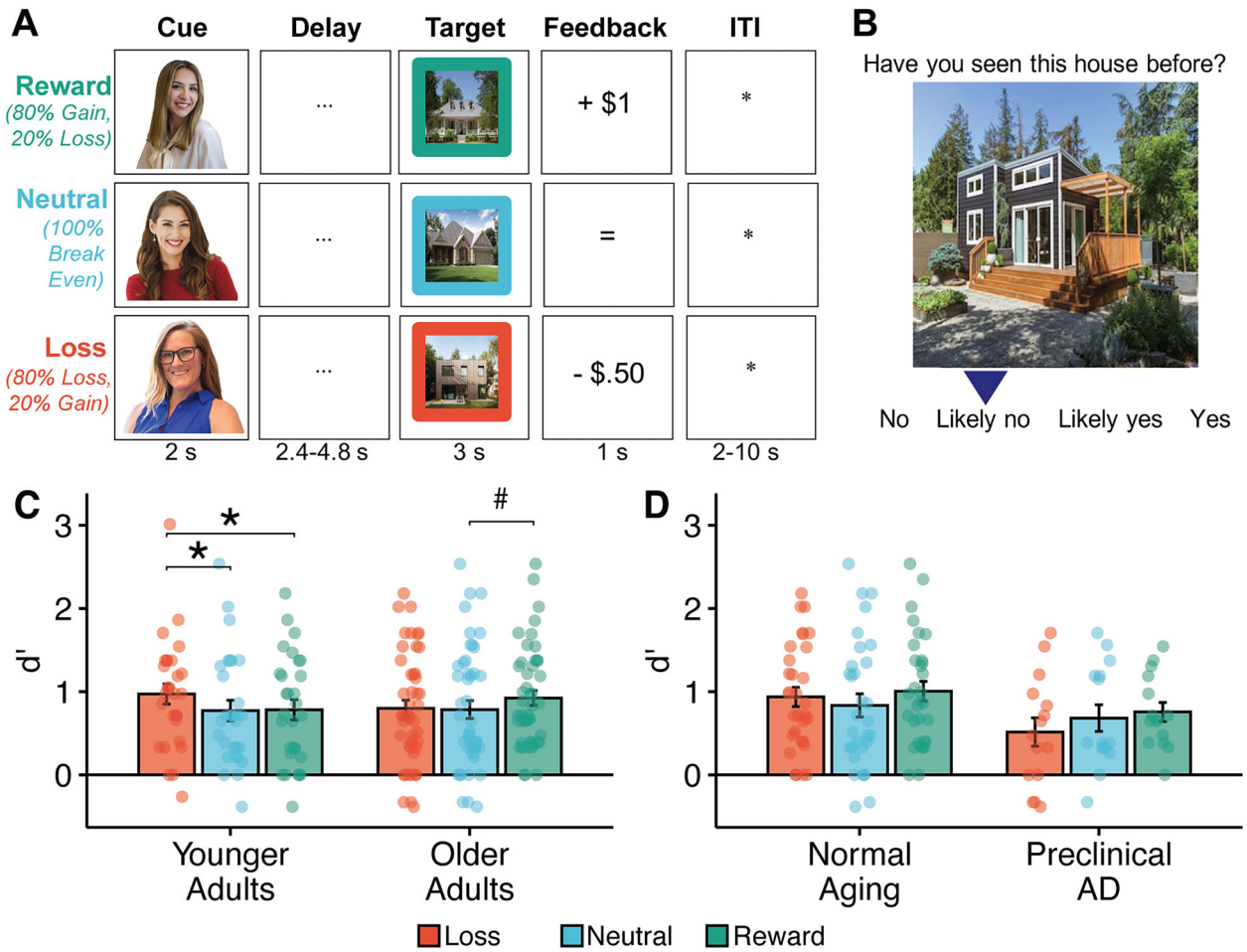

Figure 1. Behavioral task and results. ***A***, Real Estate Selling Task. During fMRI scanning, subjects completed the Real Estate Selling Task. Three trial types (Reward, Neutral, and Loss) are shown. ***B***, Subsequent memory test. Outside the scanner subjects were shown photos of houses and asked to indicate whether they had seen the house previously. ***C***, Subsequent Memory performance. Younger adults showed significantly better memory for houses shown in the loss condition compared with the neutral and reward conditions. Older adults showed better memory for houses in the reward condition compared with the neutral condition. ***D***, No effect of preclinical Alzheimer's. There was no significant difference in memory detected between the normal agers and preclinical AD biomarker groups. $^{\#}p < 0.05$, before FDR correction for multiple comparisons on post hoc pairwise *t* tests; $^{*}q < 0.05$, after FDR correction for multiple comparisons on post hoc pairwise *t* tests. Error bars represent standard error.

Memory performance was scored using d', calculated as the difference between the normalized hit rate and the normalized false alarm rate:

$$d' = z(H) - z(F),$$

where H is the proportion of previously seen house images that a subject correctly identified as remembered with high confidence ("Yes") and F is the proportion of lure house images that a subject mistakenly identified as remembered with high confidence ("Yes").

Quantification of learning performance

Learning performance was quantified as the proportion of trials during the Real Estate Selling Task where participants correctly indicated the identity of the realtor. No-response trials were treated as incorrect. Learning performance measures were calculated across all trials and for each of the three valences separately and are presented in Figure S2*a*,*b*. Though our focus is on memory outcomes, we used learning performance as a regressor of no interested to limit possible confounding effects of individual differences in task-learning performance on observed memory effects.

[^{18}F]FMT PET acquisition, reconstruction, and processing

The irreversible PET tracer [^{18}F]Fluoro-l-m-tyrosine (FMT) was used to measure dopamine synthesis capacity. [^{18}F]FMT was synthesized at Lawrence Berkeley National Laboratory, as previously described (VanBrocklin et al., 2004). The [^{18}F]FMT data have been included in previous independent analyses (Ciampa et al., 2022a; Parent et al., 2022). Participants were injected with ~2.5 mCi of [^{18}F]FMT as a bolus in an antecubital vein and scanned using a Biograph Truepoint 6 PET/CT (Siemens Medical Systems). Participants took oral carbidopa (2.5 mg/kg) ~1 h before scanning to limit the peripheral metabolism of [^{18}F]FMT. Dynamic acquisition frames were collected over a 90 min period in 3D mode (25 frames total: 5 × 1 min, 3 × 2 min, 3 × 3 min, 14 × 5 min). Reconstruction of the scans involved an ordered subset expectation maximization algorithm with weighted attenuation, correction for scatter, and smoothing with a 4 mm full-width at half-maximum (FWHM) kernel. [^{18}F]FMT data were processed using SPM12 software (http://www.fil.ion.ucl.ac.uk/spm). Images were realigned to the middle (12th) frame in order to correct for motion between frames, and the first five images were summed before realignment. PET images were coregistered to the T1-weighted structural scan using the mean of the frames corresponding to the first 20 min of data acquisition as a target. Patlak plotting was used to perform graphical analysis for irreversible tracer binding (Patlak and Blasberg, 1985) with posterior gray cerebellum as the reference region. K_i maps were generated from PET frames corresponding to 25 and 90 min (Ciampa et al., 2022a; Parent et al., 2022), which represent the amount of tracer accumulated in the brain relative to the reference region. K_i can be expressed as $K_i = k_2k_3 / (k_2 + k_3)$, where k_2 is the rate constant for the return of free [^{18}F]FMT from brain back to plasma and k_3 is the rate constant for the trapping of brain [^{18}F]FMT by aromatic amino acid decarboxylase. These images are comparable with K_i images obtained using a blood input function but are scaled to the volume of tracer distribution in the reference region; we use K_i here for simplicity. Partial volume correction (PVC) was applied to limit contributions of surrounding gray matter, white matter, and CSF to the measurement of striatal [^{18}F]FMT K_i. PVC was applied to K_i images using the Geometric Transfer Matrix approach (Rousset et al., 1998). Striatal regions of interest (ROIs) were manually drawn on each participant's T1-weighted structural scan as previously described (Mawlawi et al., 2001) using Mango software. To apply the PVC in native space, we used FreeSurfer-generated ROIs for gray matter cortical and subcortical regions, white matter, and CSF with manually drawn striatal ROIs substituting for the automated striatal segmentation. The striatal region of interest for this study was the ventral striatum (VST; Fig. 2*A*).

[^{11}C]PiB PET and [^{18}F]FTP PET acquisition, reconstruction, and preprocessing

β-amyloid (Aβ) status was determined for a subset of older adult participants using [^{11}C]Pittsburgh compound B ([^{11}C]PiB) PET ($n = 45$). Tau burden was also determined for a subset of older adult participants ($n = 41$) using [^{18}F]Flortaucipir ([^{18}F]FTP). All [^{11}C]PiB and [^{18}F]FTP scans occurred within 3 years of a subject's fMRI scan. A detailed description of PiB and FTP acquisition has been published previously (Schöll et al., 2016). After PiB injection, dynamic frames were collected for 90 min. These frames were realigned, coregistered, and resliced to the 3T structural T1. Distribution volume ratio (DVR) was calculated using a Logan graphical analysis (Logan J et al., 1990) on frames corresponding to 35–90 min postinjection using a cerebellar gray reference region and mean gray matter DVR was computed. There were 15 PiB-positive individuals in this study. [^{18}F]FTP Standardized uptake volume ratio (SUVR) images were created based on mean tracer uptake over 80–100 min postinjection, normalized using an inferior cerebellar gray reference region. As previously described, SUVR images were partial volume corrected on native space FreeSurfer-derived ROIs (Baker et al., 2017). To determine the tau status of each individual, mean SUVR values within Braak III/IV regions were extracted from each subject. A threshold of 1.26 was used to determine positive or negative tau status (Maass et al., 2017). Tau-PET analyses focused on Braak III/IV regions where pathology is likely AD rather than age-related.

MRI acquisition

Structural and functional MRI data were acquired on a 3-Tesla Siemens TIM/Trio scanner located at the Henry H. Wheeler Jr. Brain Imaging Center in Berkeley, California. A 32-channel head coil was used for all scans. Whole-brain high-resolution T1-weighted volumetric magnetization prepared rapid gradient echo image (MPRAGE) scans were acquired for each subject (voxel size, 1 mm isotropic; TR, 2,300 ms; TE, 2.98 ms; matrix, 256 × 240; sagittal plane; 160 slices). For task-based fMRI scans, T2*-weighted echoplanar images were acquired using a multiband sequence (slice acceleration factor, 4; TR, 2,400 ms; TE, 36 ms; flip angle, 45°; partial Fourier acquisition). A total of 88 slices were acquired, covering the whole brain. A total of 246 volumes were acquired with 1.54 mm isotropic voxels (matrix size 138 × 138) and the z-axis was aligned to the AC-PC line. Two opposite phase-encoded EPI fieldmaps (one anterior-to-posterior, the other posterior-to-anterior) were also collected for each subject to be used for distortion correction of the functional images (TR, 16,000 ms; TE, 111 ms; flip angle, 90°).

fMRI preprocessing with fMRIPrep

MRI preprocessing was performed using fMRIPrep (22.0.2) which is based on NiPype (1.8.5; Esteban et al., 2019). Preprocessing steps included skull stripping, distortion correction using the phase-encoded EPI fieldmaps, coregistration of each subject's functional data with their anatomical scan using boundary-based registration with six degrees of freedom, estimation of head-motion parameters, slice time correction, and spatial normalization. Full details of the reproducible fMRIPrep pipeline are described in the Supplementary Materials.

Experimental design and statistical analysis

Experimental design. In the analyses described in detail below, our primary effects of interest were subsequent memory performance (d'), dopamine synthesis capacity ([^{18}F]FMT K_i), and memory-related fMRI BOLD activation. For each of these effects, we tested for relationships with age group (younger and older adults), biomarker group (younger adults, normal agers, and preclinical AD), and trial valence (loss, neutral, and reward). Linear models were used to assess between-participant effects. Linear mixed effect models were used when investigating trial valence to account for within-subject variability.

Supplementary analyses also tested for relationships with continuous measures of tau burden ([^{18}F]FTP SUVR in Braak III/IV regions) and amyloid load ([^{11}C]PiB DVR), rather than using the discrete biomarker groups. In models of the older adult data, covariates of noninterest included age, sex, and years of education. Follow-up analyses included an additional covariate for learning performance on the task, in an effort to isolate independent effects on memory ability. In two cases, statistical significance changed following adjustment for learning, which we report in the main text and which we interpret to suggest that learning performance contributed to those memory associations being tested.

Subsequent memory analysis. We used a linear mixed effect model to test whether memory ability differed across age groups and trial valences (fixed effects), with a random effect of intercept [$d' \sim$ age_group × valence + (1 | subject)] (Fig. 1*B*). To test whether biomarker group was associated with memory ability within the older adult age group, an additional linear mixed effect model was conducted [$d' \sim$ biomarker_group × valence + (1 | subject)] (Fig. 1*C*). Post hoc pairwise *t* tests (FDR corrected for multiple comparisons) allowed us to probe the valence-specific effects that differed across age/biomarker groups.

Tests for associations with dopamine synthesis capacity. Using an independent samples *t* test, we tested for significant differences in dopamine synthesis capacity across age groups (Fig. 2*B*) and biomarker groups (see Results). We also conducted linear models to test for direct relationships between [^{18}F]FMT K_i and continuous measures of amyloid load [PiB ~ FMT + age + sex + years_edu] (Fig. 2*C*) and tau burden [FTP ~ FMT + age + sex + years_edu] (Fig. 2*D*). To investigate whether dopamine synthesis capacity was associated with memory, we compared measures of dopamine synthesis capacity to memory scores (d') for the reward, neutral, and loss conditions [$d' \sim$ biomarker_group × fmt_ki_vst + biomarker_group × valence + (1 | subject)] (Fig. 2*E*).

Whole-brain fMRI analysis. Voxelwise analysis was performed on single participant data using a general linear model (GLM) implemented with AFNI's 3dDeconvolve command. Twelve separate predictor functions were generated for each combination of trial period (cue, target), trial memory performance (remembered, forgotten), and trial valence (reward, neutral, loss). Nuisance predictors of noninterest were also generated for the cue and target periods of the "surprise" trials (e.g., when a reward realtor actually sold a house at a loss). Each predictor was also paired with an amplitude-modulated predictor to account for the confidence of a participant's memory on a given trial (regressors were weighted 1.0 for high-confidence trials and 0.5 for low-confidence trials). Each of these predictors consisted of a BLOCK basis function with length equal to the duration of the event being modeled (e.g., 2.0 s for the cue period; 3.0 s for the target period), convolved with a standard hemodynamic response function (HRF). The GLM also included six nuisance regressors per run for head motion (*x*, *y*, and *z* translations and rotations) and four-degree polynomial baseline regressors to account for per-run drift effects. The first four volumes (to account for steady-state stabilization) and high-motion volumes (>0.5 mm normed frame-to-frame distance) were censored from the GLM analysis. Subjects for whom >20% of volumes were determined to be high-motion were excluded from the analysis. The GLM was fitted using the restricted maximum likelihood method (ReML) implemented in AFNI.

Statistical images generated from the univariate GLM assigned a beta-weight to each voxel for each of the predictors-of-interest. Contrasts at the individual subject level were generated for remembered versus forgotten trials in each of the three valence conditions (reward, neutral, and loss) and during the cue and trial epochs separately. These statistical images were subsequently used as input to a linear mixed effects model for group fMRI analyses (implemented with AFNI's 3dLME command). In the linear mixed effects model, we included a random effect of intercept and fixed effects of memory (remembered vs forgotten), valence (reward, neutral, and loss), and biomarker group (young adults, normal agers, and preclinical AD). Voxelwise contrast maps highlighting regions with a main effect of memory or biomarker group on BOLD signal are shown in Figure 3*A*. Plots were created in AFNI using the "highlight don't hide" principle (Taylor et al., 2023), whereby beta-weights for statistically significant voxels (according to a strict significance threshold of $p < 0.001$) are highlighted in full color and outlined in black and nonsignificant voxels are still displayed, but with increasing opacity as the *p* value increases.

Post hoc ROI analysis of fMRI data. From the voxelwise analysis, we identified an activation cluster within parahippocampal cortex that showed a significant main effect for memory with greater activation during encoding of remembered versus forgotten trials (Fig. 3*A*). Beta-weights for the remembered versus forgotten contrast were extracted from this region for each participant to examine whether individual differences in activation were associated with biomarker group [BOLD ~ biomarker_group] (Fig. 3*B*), individual differences in memory [$d' \sim$ biomarker_group × BOLD] (Fig. 3*C*), or ventral striatal dopamine synthesis capacity [BOLD ~ fmt_vst_ki × biomarker_group + sex] (Fig. 3*D*).

Exploratory analysis of age-related valence effects. Exploratory analyses probed age group differences in the effect of valence (reward vs loss) on memory as they related to dopamine synthesis capacity. To explicitly test for valence-related memory biases across age/biomarker groups, we calculated a valence index for each participant:

$$\text{Valence Index} = \frac{H_{\text{reward}} - H_{\text{loss}}}{H_{\text{reward}} + H_{\text{loss}}},$$

where H_{valence} is defined as the hit rate for trials of each valence (reward or loss; proportion of trials where a previously shown house was correctly identified as remembered).

In our behavioral analyses, we identified a crossover interaction such that the effect of valence on memory differed for young and older adults ($b = 0.314$, $t = 2.80$, $p = 0.006$). Young adults showed better memory for loss trials compared with reward and neutral trials, but the memory-enhancing effect of loss was absent in older adults who had, on average, highest memory performance for the reward trials (Fig. 1*C*). This finding, along with prior research suggesting shifts in valence biases in aging away from negative information and toward positive information (Mather and Carstensen, 2005; Mather, 2024), motivated our exploratory analysis into whether an age-related shift in valence effects on memory was related to dopamine synthesis capacity and/or AD-related pathology.

An independent *t* test was conducted to test for differences in the valence index across age groups. Additionally, 95% confidence intervals were calculated to estimate whether the mean valence index was significantly above or below zero for each age group. We used a linear model to test whether the valence index was related to dopamine synthesis capacity across biomarker groups [valence_index ~ biomarker_group × fmt_ki_vst] (Fig. 4*B*).

Statistical analysis code and software. Data were visualized using the ggplot2 (v3.5.1) and ggpubr (v0.6.0) packages in R. Linear mixed effects models were conducted in R using the lmerTest (v3.1.3) and lme4 (v1.1.32) packages. Measures of effect size, post hoc pairwise *t* tests, and post hoc tests of slope were conducted using the emmeans (v1.10.0), rstatix (v0.7.2), and lsmeans (v2.30.2) packages. Scripts and anonymized data used to generate each of the figures and the corresponding statistical analyses are openly available at Open Science Framework (doi:10.17605/OSF.IO/SRYB9).

Results

Older age impacts the effect of reward valence on subsequent memory

To test whether memory performance across reward, neutral, and loss conditions differed between young and older adults, we conducted a linear mixed effect model with fixed effects for age group (younger adults and older adults) and trial valence (loss, neutral, and reward) and a random effect of intercept [$d' \sim$ age_group × valence + (1 | subject)]. The model demonstrated a significant crossover interaction of age group and trial valence on memory scores ($b = 0.314$, $t = 2.80$, $p = 0.006$; Fig. 1*C*). Post hoc pairwise *t* tests (with FDR correction for multiple comparisons) showed that young adults exhibited better memory for houses presented during the loss condition compared with the neutral ($t_{(29)} = 2.28$, $q = 0.049$) and reward conditions ($t_{(29)} = 2.16$, $q = 0.049$). This contrasted with the older adults for whom the memory enhancing effect of monetary loss was absent (loss vs reward $t_{(46)} = -1.79$, $q = 0.11$; loss vs neutral $t_{(46)} = 0.21$, $q = 0.84$). On average, older adults showed highest memory performance for the reward condition, though

performance was not significantly better than the loss or neutral conditions following multiple-comparisons correction (reward vs neutral: $t_{(46)} = 2.00$, $p = 0.047$, $q = 0.11$). While younger adults showed better overall learning performance on the Real Estate Selling Task compared with older adults ($b = 0.19$, $t = -4.89$, $p < 0.001$; Fig. S2*a,b*), the interaction between age group and valence on memory remained significant in a separate model that also included learning performance as a covariate ($b = 0.30$, $t = 2.65$, $p = 0.009$) though pairwise t tests probing specific valence effects within group were not significant. Additional models [performance ~ tau_burden × valence + age + sex + years_edu + (1 | subject)] found no significant effects of tau burden on memory ($b_{tau} = -1.39$, $t = 1.26$, $p = 0.27$) or learning ($b_{tau} = -0.46$, $t = -1.64$, $p = 0.11$) within the older adult cohort (Fig. S2*c–f*).

Association between memory and dopamine synthesis capacity is disrupted by AD pathology

Older adults showed significantly higher [^{18}F]FMT K_i in the ventral striatum compared with young adults ($t_{(41,14)} = 3.89$, $p < 0.001$; Fig. 2*B*), which is consistent with previous reports of apparent elevation of dopamine synthesis capacity in aging (Dejesus et al., 2001; Braskie et al., 2008; Berry et al., 2016). There was no significant difference in [^{18}F]FMT K_i between normal agers and preclinical AD biomarker groups ($t_{(28,13)} = -0.46$, $p = 0.65$) and no relationship with continuous [^{11}C]PiB DVR ($b = 0.00011$, $t = 0.51$, $p = 0.61$; Fig. 2*C*) or [^{18}F]FTP SUVR ($b = 0.0039$, $t = 1.11$, $p = 0.27$; Fig. 2*D*).

To investigate whether dopamine synthesis capacity was associated with memory, we compared measures of [^{18}F]FMT K_i in the ventral striatum to memory scores (d') for the reward, neutral, and loss conditions. We conducted a linear mixed effect model with fixed effects for the interaction between group and [^{18}F]FMT K_i in the ventral striatum, and valence and a random effect of intercept [d' ~ biomarker_group × fmt_ki_vst + biomarker_group × valence + (1 | subject)]. The model demonstrated a significant interaction between biomarker group and dopamine synthesis capacity such that preclinical AD older adults showed a significantly more negative association between ventral striatum [^{18}F]FMT K_i and d' compared with young adults ($b = -174.9$, $t = -2.42$, $p = 0.02$; Fig. 2*E*). The interaction remained significant in an additional model that included a term to control for learning performance ($b = -159.9$, $t = -2.24$, $p = 0.03$) and was also significant in a model that used continuous measures of tau burden rather than discrete biomarker groups ($b = -1011$, $t = -2.97$, $p = 0.005$). Post hoc testing with the R function "lstrends" demonstrated that the normal agers biomarker group showed a significant positive association between ventral striatum [^{18}F]FMT K_i and d' ($b = 115.5$, $t = 2.83$, $p = 0.007$). Together, these results suggest that normal agers show a youth-like positive relationship between [^{18}F]FMT K_i in the ventral striatum and memory scores. However, the presence of preclinical AD pathology disrupts this relationship.

BOLD signal in parahippocampal cortex is associated with subsequent memory

Next, we identified regions for which BOLD signal was related to subsequent memory and biomarker group. We observed a significant main effect of subsequent memory on BOLD signal during the target period (Fig. 3*A*, top row). Significant activation clusters were primarily observed in the parahippocampal cortex. These brain regions exhibited greater BOLD activation for subsequently remembered trials compared with subsequently forgotten trials (Table 2 lists activation clusters and coordinates). We also observed a significant main effect of biomarker group on BOLD signal during the target period (Fig. 3*A*, bottom three rows). Highlighted brain regions exhibited greater BOLD activation in young adults compared with normal agers and preclinical AD (Table 3 lists activation clusters and coordinates). We did not observe a significant main effect of valence or a significant valence × memory interaction effect on BOLD signal in the voxelwise analysis.

Using the activation cluster within parahippocampal cortex as a region of interest, we examined how memory-related BOLD activation was related to AD pathology and dopamine synthesis capacity. When considering only the older adult participants, parahippocampal BOLD activation mirrored patterns observed for behavioral analyses with no significant differences in memory-related activation based on biomarker group ($t_{(26,13)} = 0.92$, $p = 0.37$). Analyses including young adults showed an effect of biomarker group on memory-related BOLD activation (BOLD ~ biomarker_group), such that young adults showed greater remembered vs forgotten parahippocampal BOLD ($b = 0.105$, $t = 2.58$, $p = 0.01$). Post hoc t tests (with FDR correction for multiple comparisons) demonstrated that young adults showed significantly greater remembered versus forgotten BOLD activation in the parahippocampal ROI compared with the normal agers ($t_{(27,26)} = 2.01$, $q = 0.049$) and preclinical AD biomarker groups ($t_{(27,13)} = 2.38$, $q = 0.03$; Fig. 3*B*).

Next we used a linear model to test whether there was an interaction between biomarker group and parahippocampal BOLD activity on subsequent memory ability [d' ~ biomarker_group × BOLD]. This model showed a significant interaction between parahippocampal BOLD activation and biomarker group on memory ($b = -6.25$, $t = -2.78$, $p = 0.007$) such that young adults and normal agers showed a positive relationship between BOLD signal and memory (young adults: $b = 4.94$, $t = 3.63$, $p < 0.001$; normal agers: $b = 4.65$, $t = 2.972$, $p = 0.004$), but the preclinical AD group did not (preclinical AD: $b = -1.31$, $t = -0.731$, $p = 0.47$; Fig. 3*C*). The interaction effect remained significant when including a term to account for individual differences in learning performance ($b = -0.07$, CI = [−0.11, −0.02], $p = 0.003$).

We also used a linear model to test whether there was an interaction between ventral striatal dopamine synthesis capacity and biomarker group on fMRI activation in the parahippocampal cortex [BOLD ~ biomarker_group × fmt_ki_vst] (Fig. 3*D*). This model demonstrated that dopamine synthesis capacity was significantly related to fMRI signal in young adults ($b = 26.34$, $t = 2.06$, $p = 0.045$). Additionally, there was a significant interaction between [^{18}F]FMT K_i and biomarker group when comparing the preclinical AD and young adult groups ($b = -38.64$, $t = -2.32$, $p = 0.03$). Supplementary analyses that used continuous measures of tau burden rather than discrete biomarker groups also demonstrated a significant interaction, such that higher tau burden was associated with a more negative relationship between dopamine synthesis capacity and parahippocampal BOLD signal ($b = -164.4$, $t = -2.21$, $p = 0.04$). In additional supplementary analyses that included learning performance as a covariate, the interaction effect was no longer significant ($b = -89.5$, $t = -1.15$, $p = 0.26$), but there was still a positive relationship between [^{18}F]FMT K_i and memory in young adults ($b = 25.76$, $t = 2.08$, $p = 0.04$).

Altogether, these results suggest that parahippocampal activation is associated with successful memory performance and dopamine synthesis capacity in young adults, but these relationships wain with older age and are particularly attenuated in the presence of preclinical AD pathology.

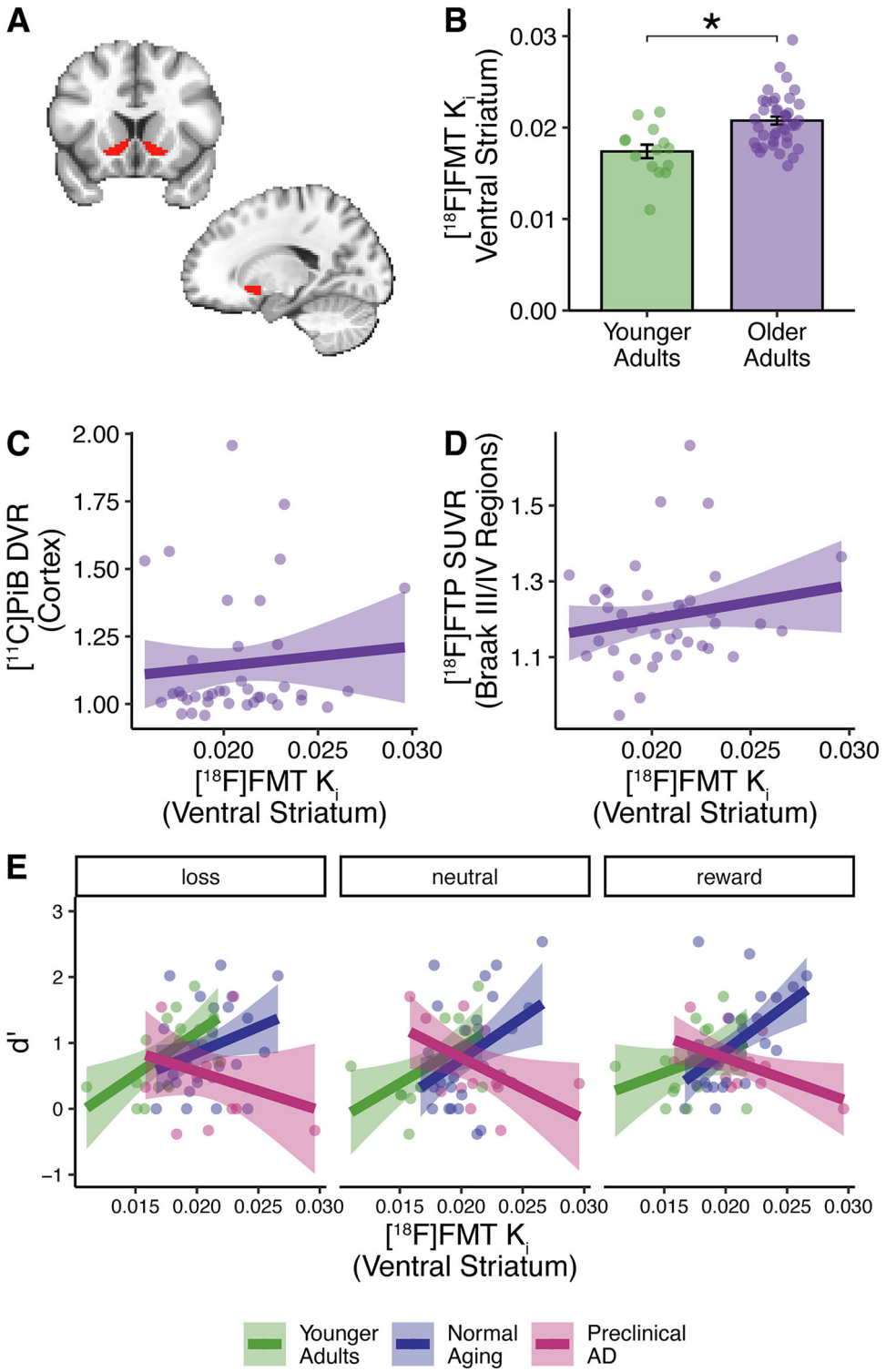

Figure 2. Dopamine synthesis capacity in the ventral striatum is associated with memory in a pathology-dependent manner. ***A***, Ventral striatum ROI. To measure dopamine synthesis capacity, [^{18}F]FMT K_i was quantified in the ventral striatum (red). ***B***, Age effect on dopamine synthesis capacity. Older adults (purple) showed increased levels of dopamine synthesis capacity compared with younger adults (green) in the ventral striatum. (Error bars show standard error). ***C***, No relationship with amyloid load. A linear model found no significant relationship between [^{18}F]PiB DVR in cortical gray matter and [^{18}F]FMT in the ventral striatum. [FMT ~ pib_dvr + age + sex + years_edu] ($b = 0.00073$, $t = 0.36$, $p = 0.72$). ***D***, No relationship with tau burden. A linear model found no significant relationship between [^{18}F]FTP SUVR in Braak III/IV regions and [^{18}F]FMT in the ventral striatum. [FMT ~ tau_burden + age + sex + years_edu] ($b = 0.0034$, $t = 0.94$, $p = 0.35$). ***E***, AD pathology disrupts relationship with memory. In younger adults (green) and normally aging older adults (blue), increased dopamine synthesis capacity was associated with better memory across conditions. Older adults with preclinical Alzheimer's pathology (pink) show a disruption in this relationship. (Lines show linear fit; shaded regions show 90% confidence interval).

Valence effects on memory are associated with dopamine synthesis capacity

In our behavioral analyses, we identified a crossover interaction where young adults showed better memory for loss trials relative to reward, but this effect was altered in older adults (Fig. 1*C*). This impact of age on valence effects is broadly consistent with previously reported memory biases in older age (Mather and Carstensen, 2005). To explicitly test whether age-related changes

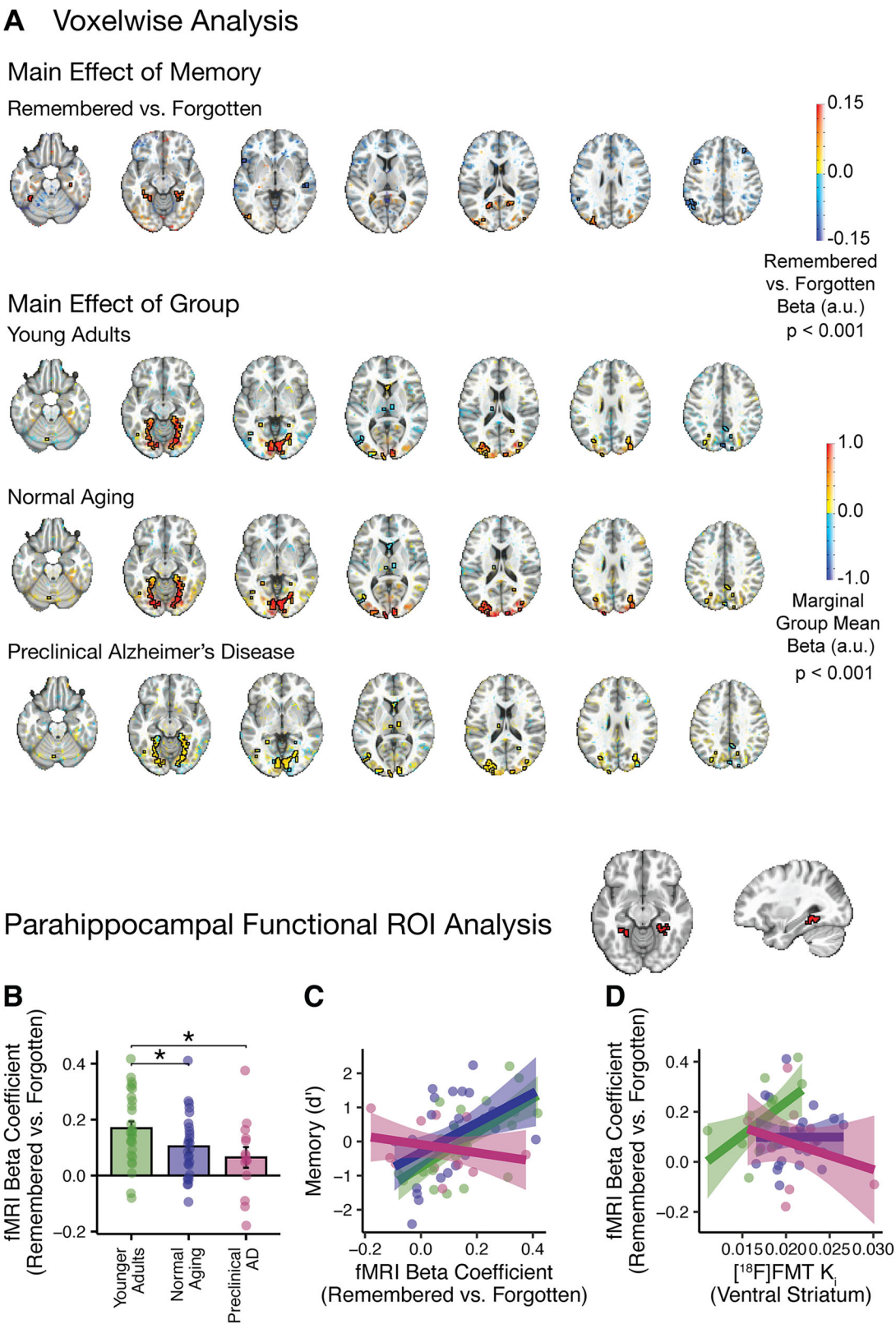

Figure 3. Subsequent memory for house stimuli was associated with parahippocampal activation, which was reduced in older adults. ***A***, Effects of memory and biomarker group on fMRI activation. We observed an overall main effect of memory (remembered vs forgotten) on BOLD signal (top row). We also observed a main effect of biomarker group on BOLD signal (bottom three rows). We did not observe a significant main effect of valence or significant interactions at the voxel level. Model: [BOLD ~ memory × valence × biomarker_group]. Voxelwise maps are presented according to the "highlight don't hide" philosophy (Taylor et al., 2023). Black outlines denote voxels showing a significant main effect of memory (top row) or main effect of biomarker group (bottom three rows) at $p < 0.001$. Opacity is reduced as p value increases. ***B***, Age and AD pathology disrupt parahippocampal activation. Region-of-interest analysis used clusters in parahippocampal cortices that showed a significant main effect of memory. Signal is significantly greater in the young adult group compared with normal agers and preclinical AD biomarker groups. ***C***, Individual differences in parahippocampal activation are related to memory. In younger adults and normal agers, the magnitude of parahippocampal BOLD activity for remembered versus forgotten items is associated with overall memory performance, but this is not the case for the preclinical AD biomarker group. ***D***, Dopamine synthesis capacity related to parahippocampal

Table 2. Clusters showing a main effect of memory on BOLD signal across the entire cohort

X	Y	Z	# Vox.	Peak (Z)	Region
−56.5	−48.5	29.5	119	−4.47	L Supramarginal G.
23.5	−38.5	−14.5	72	4.26	R Parahippocampal G.
7.5	−56.5	9.5	71	3.70	R Retrosplenial
−22.5	−44.5	−16.5	59	4.30	L Parahippocampal G.
−32.5	−92.5	21.5	53	3.66	L Supramarginal G.
−42.5	15.5	35.5	22	−4.58	L Middle Frontal G.
−36.5	−50.5	−22.5	18	3.80	L Fusiform G.
45.5	−86.5	13.5	18	4.21	R Lateral Occipital G.
−14.5	−60.5	17.5	18	3.44	L Retrosplenial
−32.5	−36.5	−16.5	16	4.63	L Parahippocampal G.
25.5	−84.5	47.5	16	3.58	R Intraparietal S.
33.5	−68.5	−34.5	16	−4.28	R Cerebellum

X, Y, Z, coordinates in MNI template space; Vox., voxel; L, left; R, right; G, gyrus; S, sulcus.

Table 3. Clusters showing a main effect of biomarker group on BOLD signal across the entire cohort

X	Y	Z	# Vox.	Peak (X^2)	Region
−29.5	56.5	−6.5	855	15.5	R Parahippocampal G.
26.5	82.5	17.5	306	14.3	L Superior Occipital G.
30.5	50.5	−6.5	243	27.1	L Fusiform G.
−29.5	86.5	23.5	137	16.2	R Middle Occipital G.
0.5	64.5	41.5	73	19.7	L Precuneus
28.5	76.5	27.5	57	14.7	L Middle Occipital G.
44.5	72.5	−10.5	56	14.4	L Inferior Occipital G.
−1.5	84.5	37.5	47	15.5	R Superior Parietal Lobule
6.5	20.5	9.5	40	20.4	L Thalamus
6.5	78.5	55.5	40	16.1	L Superior Parietal Lobule
−11.5	98.5	13.5	33	14.0	R Cuneus
−37.5	68.5	−16.5	29	15.7	R Fusiform G.
42.5	74.5	1.5	29	16.3	L Middle Occipital G.
−1.5	−17.5	7.5	28	17.3	L Caudate
−35.5	88.5	11.5	27	15.0	R Middle Occipital G.
−13.5	66.5	37.5	25	16.1	R Cuneus
0.5	76.5	−30.5	20	15.5	L Cerebellum
4.5	78.5	−18.5	13	21.2	L Cerebellum
52.5	24.5	25.5	11	18.6	L Supramarginal G.
−15.5	88.5	37.5	11	15.1	R Cuneus
26.5	70.5	51.5	11	20.9	L Superior Parietal Lobule

X, Y, Z, coordinates in MNI template space; Vox., voxel; L, left; R, right; G, gyrus; S, sulcus.

in memory biases were related dopamine and/or AD biomarkers, we calculated a valence index for each participant to capture the degree to which their memory was biased for houses paired with reward versus loss outcomes (see Materials and Methods). We found a significant age group difference in the valence index such that older adults showed a memory bias for reward while young adults showed a memory bias for loss ($t_{(29,43)} = 3.33$, $p = 0.002$; Fig. 4*A*). Moreover 95% confidence intervals were above zero [0.0012, 0.21] for older adults, and below zero [−0.30, −0.046] for younger adults, indicating significant valence biases within each age group. We hypothesized that these shifts in valence biases may be related to levels of dopamine synthesis capacity ([^{18}F]FMT K_i) in the ventral striatum, which is significantly higher in older adults relative to young. To test this hypothesis, we used a linear model to compare the relationship between the valence index and [^{18}F]FMT K_i in the ventral striatum across biomarker groups [valence_index ~ group × fmt_ki_vst]. The model identified a significant interaction between biomarker group and ventral striatum [^{18}F]FMT K_i such that both normal agers ($b = 0.20$, $t = 2.24$, $p = 0.03$) and preclinical AD biomarker groups ($b = 0.43$, $t = 4.04$, $p < 0.001$) showed a significantly more positive relationship between [^{18}F]FMT K_i and the valence index when compared with young adults (Fig. 4*B*). Post hoc tests using the R package "lstrends" confirmed that older adults as a whole showed a significantly positive relationship between ventral striatum [^{18}F]FMT K_i and valence index ($b = 41.6$, 95% CI = [3.21, 79.9]). The interaction effect remained significant in a follow-up analysis that accounted for individual differences in learning performance on reward versus loss trials ($b = 90.4$, $t = 2.17$, $p = 0.04$). Analyses using continuous measures of tau burden extend these findings to suggest that high levels of tau pathology may further enhance positive memory biases in aging. A significant interaction showed the strongest relationship between valence index and dopamine synthesis capacity for high tau individuals ($b = 453.8$, $t = 2.23$, $p = 0.03$; Fig. S3).

Discussion

This study investigated the joint influences of dopamine synthesis capacity and AD pathology on reward-related memory in aging. In young adults, we found clear associations between higher ventral striatal dopamine, memory, and medial temporal lobe activation, which are highly consistent with proposals that dopamine modulates the encoding of motivationally significant events (Shohamy and Adcock, 2010). In older adults, these associations were modified. When considered independently, neither dopamine synthesis capacity nor AD pathology alone explained individual differences in memory performance. Instead, we observed an interaction between these two age-related brain features. While normal aging was associated with preservation of "youth-like" dopamine–cognition associations, AD-related pathology disrupted these relationships. Replicating previous findings, dopamine synthesis capacity was significantly higher in older relative to young adults (Braskie et al., 2008; Berry et al., 2016; Ciampa et al., 2022b) and was not directly related to pathology burden. Our exploratory analyses link elevation in this dopamine marker with reward valence effects on memory, which are modified in older age (Samanez-Larkin and Knutson, 2015), and provide initial support that age-related changes in neuromodulator systems contribute to affective memory biases across the lifespan.

Young adult performance and associations with dopamine synthesis capacity and brain activation are highly consistent with prior research, providing a foundation to interpret alterations in older age. In young adults, successful encoding was associated with higher temporal lobe activation, including parahippocampal cortex regions implicated in the visual processing of house stimuli (Epstein and Kanwisher, 1998), and often identified in subsequent memory analyses (Kim, 2011; Chowdhury et al., 2012), including incidental encoding paradigms with monetary incentives (Erk et al., 2003; Adcock et al., 2006). Despite a limited number of young participants completing PET imaging, we identified a strong positive association between dopamine synthesis capacity and both higher memory performance and

←

activation in young adults. While younger adults show a positive relationship between [^{18}F]FMT K_i in the ventral striatum and memory-related fMRI signal in the parahippocampal cortex, the preclinical AD biomarker group shows a significantly more negative trend, with a significant interaction between biomarker group and [^{18}F]FMT *Ki* ($p < 0.05$). (Lines show linear fit; shaded regions show 90% confidence interval.)

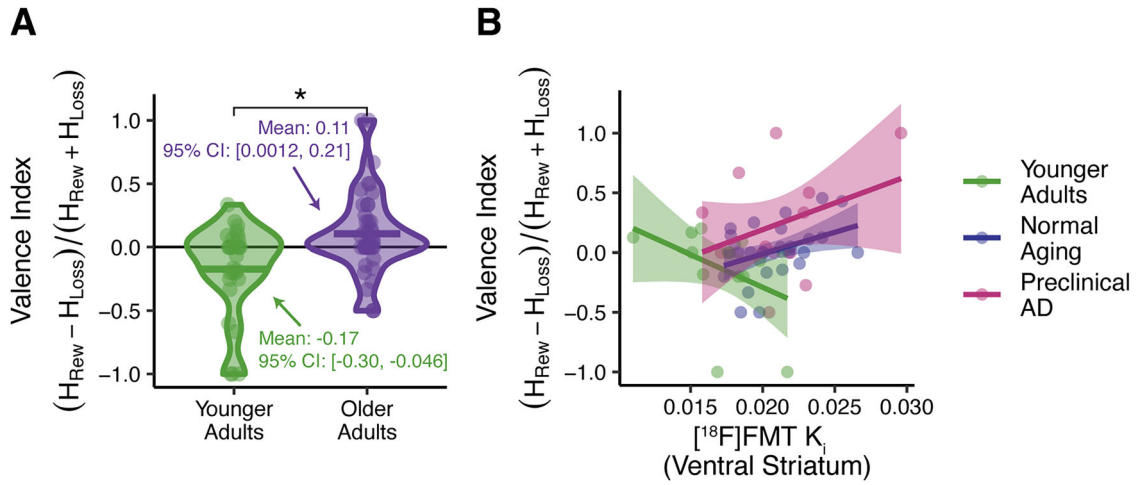

Figure 4. ***A***, Age-related valence index. Older adults (purple) showed a significantly more positive valence index compared with younger adults (green). 95% confidence intervals (CI) are below zero for younger adults and above zero for older adults. ***B***, Valence index related to dopamine synthesis capacity. In younger adults (green) [^{18}F]FMT K_i showed a negative relationship with valence index, but both normal agers and preclinical AD showed a positive relationship. (Lines show linear fit; shaded areas indicate 90% confidence interval.)

parahippocampal activation. These findings complement previous pharmacological work linking dopamine augmentation with enhanced memory performance (Chowdhury et al., 2012; Linssen et al., 2014) and a simultaneous MR/PET study linking reward-related dopamine release with increased medial temporal lobe activation (Schott et al., 2008). Further, the parahippocampal cortex receives direct and indirect dopaminergic modulation from the ventral tegmental area and ventral striatum and is ideally positioned to integrate motivationally salient information into the context of episodic memories during encoding (Haber and Fudge, 1997; Broussard et al., 2016; Tsetsenis et al., 2021; Sayegh et al., 2024). Together our findings in young adults are consistent with a framework in which higher dopamine synthesis capacity supports memory through the enhancement of temporal lobe activation during encoding.

AD-related pathology disrupted associations between higher dopamine synthesis capacity and behavior, which remained intact in normal aging. The incorporation of AD biomarkers in this study allowed us to identify diverging dopamine–cognition relationships between aging subgroups, which would have otherwise been masked. Unfortunately, most studies focused on dopaminergic mechanisms of cognitive decline in aging have not been able to account for the 20–30% of their sample that would be expected to meet criteria for preclinical AD (Nevalainen et al., 2015). These limitations have likely contributed to weakened or null results (Juarez et al., 2019), as behavior appears to be relatively decoupled from the dopamine system in the context of AD pathology. Future empirical testing of the proposal that dopaminergic changes mediate age-related cognitive decline would benefit from the incorporation of PET or fluid AD biomarkers to specifically test these effects in normal aging. Notably, both normal agers and preclinical AD biomarker groups showed an apparent loss of associations between dopamine and memory-related fMRI activation. In our biomarker group of normal agers, it is possible other sources of individual differences in fMRI activation (e.g., white matter integrity, perfusion, subclinical pathology) obscured direct relationships with dopamine in this small sample. The impact of neuropathology on hemodynamic response functions underlying fMRI activation measures is understudied and may contribute to heterogeneity in aging results and loss of clear coupling between brain measures and behavior. The use of a canonical hemodynamic response function in the current study is a limitation. Future work in larger samples should clarify how Aβ and tau burden impact hemodynamic responses (Asemani et al., 2017; West et al., 2019; Wang et al., 2025). Further, emerging fMRI research in young adults suggests the latency of hemodynamic responses is influenced by dopamine physiology (Ballard et al., 2025), but these relationships have not been investigated in aging. Together, these lines of future work are needed to characterize the impact of individual differences in pathology and endogenous dopamine on hemodynamic responses, neural-vascular coupling, and cognition.

There is consistent evidence that dopamine synthesis capacity, as indexed by higher activity of AADC, is elevated in older adults relative to young (Dejesus et al., 2001; Braskie et al., 2008; Berry et al., 2016; Karrer et al., 2017). Elevation in dopamine synthesis capacity in animal models occurs in response to neural insult (Zigmond et al., 1990; Greenwood et al., 1991) and has been interpreted to reflect compensatory processes with complementary findings in human aging (Ciampa et al., 2022b) and in early stages of Parkinson's disease (Lee et al., 2000). In the present study, elevation in dopamine synthesis did not appear to be a direct consequence of AD pathology, as these measures were not positively correlated. Instead, elevated dopamine synthesis capacity appears to be a more general feature of aging. Is elevated dopamine synthesis a good thing? In the context of an AD brain, it appears the answer is "no." Higher pathologic burden in preclinical AD appeared to disrupt and even reverse the direction of relationships between ventral striatal dopamine synthesis capacity and both cognition and brain activity. We do not yet know the mechanisms by which increased dopamine synthesis drives reduced neural activity and poorer performance in this population. One possibility is that pathology causes alterations in the physiological health of neurons that receive dopaminergic inputs, which are thus more likely to show dysregulated or dampened responses, broadly consistent with Yerkes–Dodson-like overdose effects (Cools and Robbins, 2004; Cools and D'Esposito, 2011). There is an acute need for research clarifying how the emergence of AD pathology alters the function of neuromodulator systems.

Efforts to connect age-related elevation in dopamine synthesis to augmented or transformed patterns of behavior relative to

young adults have been largely inconclusive. Our exploratory analyses suggest this dopamine marker may be relevant to understanding age-related valence effects on behavior (sometimes referred to as the "positivity effect" in aging). Memory performance in young adults suggested preferential sensitivity to monetary loss relative to reward, whereas older adults showed a reversal of this pattern. In line with our findings, previous work in young adults suggests pharmacologically enhancing dopamine shifts learning biases toward reward and away from punishment (van der Schaaf et al., 2013). Although early characterizations of the "positivity effect" have long suggested affective shifts arise from age-related changes in motivation (Mather and Carstensen, 2005; Reed and Carstensen, 2012), the field has struggled to identify neural mechanisms underlying these shifts. More recent theoretical work has proposed that the positivity effect may arise via altered balance among receptor subtypes or pre- and postsynaptic components in the dopamine system in older age (Berry et al., 2019) or through compensatory brain activity meant to counteract hyperactivation of the noradrenergic arousal systems in older age (Mather, 2024). Our data suggest elevated dopamine synthesis capacity in aging may underlie greater biases in memory for rewarded items rather than loss items. While these effects were independent of AD status (i.e., Aβ positivity), we identified a moderating impact of higher tau pathology, which warrants further investigation. While positive memory biases have been considered a general feature of aging (Mather, 2016), other research suggests effects are limited to older adults with subtle/subclincial memory impairment (Leal et al., 2016), though this prior research has not incorporated pathology biomarkers.

The present study is among the first to assess interactive effects of AD pathology and age-related dopamine changes on memory performance and task-related fMRI activation. Notable previous research has examined associations among multiple dopamine PET markers, Aβ, and structural MR measures in aging (Rieckmann et al., 2016). While limited in sample size, the current study's in vivo assessment of the dopamine system and both Aβ and tau pathology within the same individuals provides rare insight into the neurobiological drivers of motivated memory. These data suggest that changes in the dopamine system are not a proxy for AD pathological processes but that it is critical to consider the two pathways together. Recent methodological breakthroughs in AD blood plasma biomarker research (Hansson, 2021; Zetterberg and Bendlin, 2021; Ossenkoppele et al., 2022; Salvadó et al., 2023) and MRI methods for assessing catecholamine systems (Liu et al., 2019; Trujillo et al., 2019; Dahl et al., 2022) promise to accelerate our understanding of interactions between these systems and their impact on high level cognition. Expanding the field of AD-relevant research to embrace cognitive neuroscience paradigms and perspectives promises to directly support the development of sensitive behavioral measures for the early detection of AD (Berron et al., 2018; Maass et al., 2019), while shedding light on the neural basis of age and disease-related shifts in complex thought, affect, and decision-making.

References

Adcock RA, Thangavel A, Whitfield-Gabrieli S, Knutson B, Gabrieli JDE (2006) Reward-motivated learning: mesolimbic activation precedes memory formation. Neuron 50:507–517.

Asemani D, Morsheddost H, Shalchy MA (2017) Effects of ageing and Alzheimer disease on haemodynamic response function: a challenge for event-related fMRI. Healthc Technol Lett 4:109–114.

Bäckman L, Nyberg L, Lindenberger U, Li S-C, Farde L (2006) The correlative triad among aging, dopamine, and cognition: current status and future prospects. Neurosci Biobehav Rev 30:791–807.

Bäckman L, Lindenberger U, Li S-C, Nyberg L (2010) Linking cognitive aging to alterations in dopamine neurotransmitter functioning: recent data and future avenues. Neurosci Biobehav Rev 34:670–677.

Baker SL, Maass A, Jagust WJ (2017) Considerations and code for partial volume correcting [18F]-AV-1451 tau PET data. Data Brief 15:648–657.

Ballard IC, Pappas I, Furman DJ, Berry AS, deB Frederick B, White RL, Kayser AS, Jagust WJ, D'Esposito M (2025) Temporal fMRI dynamics map dopamine physiology. bioRxiv 2025.03.24.645022.

Berron D, Neumann K, Maass A, Schütze H, Fliessbach K, Kiven V, Jessen F, Sauvage M, Kumaran D, Düzel E (2018) Age-related functional changes in domain-specific medial temporal lobe pathways. Neurobiol Aging 65:86–97.

Berry AS, Shah VD, Baker SL, Vogel JW, O'Neil JP, Janabi M, Schwimmer HD, Marks SM, Jagust WJ (2016) Aging affects dopaminergic neural mechanisms of cognitive flexibility. J Neurosci 36:12559–12569.

Berry AS, Jagust WJ, Hsu M (2019) Age-related variability in decision-making: insights from neurochemistry. Cogn Affect Behav Neurosci 19:415–434.

Braskie MN, Wilcox CE, Landau SM, O'Neil JP, Baker SL, Madison CM, Kluth JT, Jagust WJ (2008) Relationship of striatal dopamine synthesis capacity to age and cognition. J Neurosci 28:14320–14328.

Broussard JI, et al. (2016) Dopamine regulates aversive contextual learning and associated in vivo synaptic plasticity in the hippocampus. Cell Rep 14:1930–1939.

Chowdhury R, Guitart-Masip M, Bunzeck N, Dolan RJ, Duzel E (2012) Dopamine modulates episodic memory persistence in old age. J Neurosci 32:14193–14204.

Ciampa CJ, et al. (2022a) Associations among locus coeruleus catecholamines, tau pathology, and memory in aging. Neuropsychopharmacol 47:1106–1113.

Ciampa CJ, Parent JH, Lapoint MR, Swinnerton KN, Taylor MM, Tennant VR, Whitman AJ, Jagust WJ, Berry AS (2022b) Elevated dopamine synthesis as a mechanism of cognitive resilience in aging. Cereb Cortex 32:2762–2772.

Cools R, D'Esposito M (2011) Inverted-U-shaped dopamine actions on human working memory and cognitive control. Biol Psychiatry 69:e113–125.

Cools R, Robbins TW (2004) Chemistry of the adaptive mind. Phil Trans A Math Phys Eng Sci 362:2871–2888.

Dahl MJ, et al. (2022) Locus coeruleus integrity is related to tau burden and memory loss in autosomal-dominant Alzheimer's disease. Neurobiol Aging 112:39–54.

Dejesus OT, Endres CJ, Shelton SE, Nickles RJ, Holden JE (2001) Noninvasive assessment of aromatic L-amino acid decarboxylase activity in aging rhesus monkey brain in vivo. Synapse 39:58–63.

Epstein R, Kanwisher N (1998) A cortical representation of the local visual environment. Nature 392:598–601.

Erk S, Kiefer M, Grothe JO, Wunderlich AP, Spitzer M, Walter H (2003) Emotional context modulates subsequent memory effect. NeuroImage 18:439–447.

Esteban O, et al. (2019) fMRIPrep: a robust preprocessing pipeline for functional MRI. Nat Methods 16:111–116.

Folstein MF, Folstein SE, McHugh PR (1975) Mini-mental state. A practical method for grading the cognitive state of patients for the clinician. J Psychiatr Res 12:189–198.

Greenwood CE, Tatton WG, Seniuk NA, Biddle FG (1991) Increased dopamine synthesis in aging substantia Nigra neurons. Neurobiol Aging 12:557–565.

Haber SN, Fudge JL (1997) The primate substantia nigra and VTA: integrative circuitry and function. CRN 11 Available at: https://www.dl.begellhouse.com/journals/7b004699754c9fe6,7f6548a676a88ce8,134b883e6fd734d7.html [Accessed December 20, 2024].

Hansson O (2021) Biomarkers for neurodegenerative diseases. Nat Med 27:954–963.

Jack Jr CR, et al. (2024) Revised criteria for diagnosis and staging of Alzheimer's disease: Alzheimer's association workgroup. Alzheimer's Dement 20:5143–5169.

Jansen WJ, et al. (2015) Prevalence of cerebral amyloid pathology in persons without dementia. JAMA 313:1924–1924.

Juarez EJ, et al. (2019) Reproducibility of the correlative triad among aging, dopamine receptor availability, and cognition. Psychol Aging 34:921–932.

Karalija N, et al. (2024) Longitudinal support for the correlative triad among aging, dopamine D2-like receptor loss, and memory decline. Neurobiol Aging 136:125–132.

Karrer TM, Josef AK, Mata R, Morris ED, Samanez-Larkin GR (2017) Reduced dopamine receptors and transporters but not synthesis capacity in normal aging adults: a meta-analysis. Neurobiol Aging 57: 36–46.
Kim H (2011) Neural activity that predicts subsequent memory and forgetting: a meta-analysis of 74 fMRI studies. NeuroImage 54:2446–2461.
Landau SM, et al. (2024) Individuals with Alzheimer's disease and low tau burden: characteristics and implications. Alzheimer's Dement 20:2113–2127.
Leal SL, Noche JA, Murray EA, Yassa MA (2016) Positivity effect specific to older adults with subclinical memory impairment. Learn Mem 23:415–421.
Lee CS, et al. (2000) In vivo positron emission tomographic evidence for compensatory changes in presynaptic dopaminergic nerve terminals in Parkinson's disease. Ann Neurol 47:493–503.
Li S-C, Rieckmann A (2014) Neuromodulation and aging: implications of aging neuronal gain control on cognition. Curr Opin Neurobiol 29: 148–158.
Linssen AMW, Sambeth A, Vuurman EFPM, Riedel WJ (2014) Cognitive effects of methylphenidate and levodopa in healthy volunteers. Eur Neuropsychopharmacol 24:200–206.
Liu KY, et al. (2019) In vivo visualization of age-related differences in the locus coeruleus. Neurobiol Aging 74:101–111.
Logan J, et al. (1990) Graphical analysis of reversible radioligand binding from time—activity measurements applied to [N-11C-methyl]-(−)-cocaine PET studies in human subjects. J Cereb Blood Flow Metab 10: 740–747.
Maass A, Landau S, Baker SL, Horng A, Lockhart SN, La Joie R, Rabinovici GD, Jagust WJ (2017) Comparison of multiple tau-PET measures as biomarkers in aging and Alzheimer's disease. NeuroImage 157:448–463.
Maass A, Lockhart SN, Harrison TM, Bell RK, Mellinger T, Swinnerton K, Baker SL, Rabinovici GD, Jagust WJ (2018) Entorhinal Tau pathology, episodic memory decline, and neurodegeneration in aging. J Neurosci 38:530–543.
Maass A, et al. (2019) Alzheimer's pathology targets distinct memory networks in the ageing brain. Brain 142:2492–2509.
Mather M (2016) The affective neuroscience of aging. Ann Rev Psychol 67: 213–238.
Mather M (2024) The emotion paradox in the aging body and brain. Annals of the New York Academy of Sciences Available at: https://onlinelibrary.wiley.com/doi/abs/10.1111/nyas.15138 [Accessed May 31, 2024].
Mather M, Carstensen LL (2005) Aging and motivated cognition: the positivity effect in attention and memory. Trends Cogn Sci 9:496–502.
Mather M, Schoeke A (2011) Positive outcomes enhance incidental learning for both younger and older adults. Front Neurosci 5:1–10.
Mawlawi O, et al. (2001) Imaging human mesolimbic dopamine transmission with positron emission tomography: I. Accuracy and precision of D_2 receptor parameter measurements in ventral striatum. J Cereb Blood Flow Metab 21:1034–1057.
Murty VP, Dickerson KC (2016) Motivational influences on memory. In: *Advances in motivation and achievement* (Kim S, Reeve J, Bong M, eds), pp 203–227. Bingley, UK: Emerald Group Publishing Limited. Available at: https://www.emerald.com/insight/content/doi/10.1108/S0749-742320160000019019/full/html [Accessed January 31, 2024].
Nevalainen N, Riklund K, Andersson M, Axelsson J, Ögren M, Lövdén M, Lindenberger U, Bäckman L, Nyberg L (2015) COBRA: a prospective multimodal imaging study of dopamine, brain structure and function, and cognition. Brain Res 1612:83–103.
Ossenkoppele R, van der Kant R, Hansson O (2022) Tau biomarkers in Alzheimer's disease: towards implementation in clinical practice and trials. Lancet Neurol 21:726–734.
Parent JH, Ciampa CJ, Harrison TM, Adams JN, Zhuang K, Betts MJ, Maass A, Winer JR, Jagust WJ, Berry AS (2022) Locus coeruleus catecholamines link neuroticism and vulnerability to tau pathology in aging. NeuroImage 263:119658.
Patlak CS, Blasberg RG (1985) Graphical evaluation of blood-to-brain transfer constants from multiple-time uptake data. J Cereb Blood Flow Metab 5:584–590.
Reed AE, Carstensen LL (2012) The theory behind the age-related positivity effect. Front Psychol 3:339.
Rieckmann A, Karlsson S, Karlsson P, Brehmer Y, Fischer H, Farde L, Nyberg L, Bäckman L (2011) Dopamine D1 receptor associations within and between dopaminergic pathways in younger and elderly adults: links to cognitive performance. Cereb Cortex 21:2023–2032.
Rieckmann A, Hedden T, Younger AP, Sperling RA, Johnson KA, Buckner RL (2016) Dopamine transporter availability in clinically normal aging is associated with individual differences in white matter integrity. Hum Brain Mapp 37:621–631.
Rousset OG, Ma Y, Evans AC (1998) Correction for partial volume effects in PET: principle and validation. J Nucl Med 39:904–911.
Salvadó G, et al. (2023) Specific associations between plasma biomarkers and postmortem amyloid plaque and tau tangle loads. EMBO Mol Med 15: e17123.
Samanez-Larkin GR, Knutson B (2015) Decision making in the ageing brain: changes in affective and motivational circuits. Nat Rev Neurosci 16:278–289.
Sayegh FJP, Mouledous L, Macri C, Pi Macedo J, Lejards C, Rampon C, Verret L, Dahan L (2024) Ventral tegmental area dopamine projections to the hippocampus trigger long-term potentiation and contextual learning. Nat Commun 15:4100.
Schöll M, et al. (2016) PET imaging of tau deposition in the aging human brain. Neuron 89:971–982.
Schott BH, et al. (2008) Mesolimbic functional magnetic resonance imaging activations during reward anticipation correlate with reward-related ventral striatal dopamine release. J Neurosci 28:14311–14319.
Shohamy D, Adcock RA (2010) Dopamine and adaptive memory. Trends Cogn Sci 14:464–472.
Spaniol J, Schain C, Bowen HJ (2014) Reward-enhanced memory in younger and older adults. J Gerontol Ser B 69:730–740.
Taylor PA, Reynolds RC, Calhoun V, Gonzalez-Castillo J, Handwerker DA, Bandettini PA, Mejia AF, Chen G (2023) Highlight results, don't hide them: enhance interpretation, reduce biases and improve reproducibility. Neuroimage 274:120138.
Trujillo P, Petersen KJ, Cronin MJ, Lin Y-C, Kang H, Donahue MJ, Smith SA, Claassen DO (2019) Quantitative magnetization transfer imaging of the human locus coeruleus. Neuroimage 200:191–198.
Tsetsenis T, Badyna JK, Wilson JA, Zhang X, Krizman EN, Subramaniyan M, Yang K, Thomas SA, Dani JA (2021) Midbrain dopaminergic innervation of the hippocampus is sufficient to modulate formation of aversive memories. Proc Natl Acad Sci U S A 118:e2111069118.
VanBrocklin HF, Blagoev M, Hoepping A, O'Neil JP, Klose M, Schubiger PA, Ametamey S (2004) A new precursor for the preparation of 6-[18F] Fluoro-l-m-tyrosine ([18F]FMT): efficient synthesis and comparison of radiolabeling. Appl Radiat Isot 61:1289–1294.
van den Bosch R, Hezemans FH, Määttä JI, Hofmans L, Papadopetraki D, Verkes R-J, Marquand AF, Booij J, Cools R (2023) Evidence for absence of links between striatal dopamine synthesis capacity and working memory capacity, spontaneous eye-blink rate, and trait impulsivity (Büchel C, Mehta M, Zald D, eds). eLife 12:e83161.
van der Schaaf ME, Fallon SJ, ter Huurne N, Buitelaar J, Cools R (2013) Working memory capacity predicts effects of methylphenidate on reversal learning. Neuropsychopharmacol 38:2011–2018.
Villeneuve S, et al. (2015) Existing Pittsburgh compound-B positron emission tomography thresholds are too high: statistical and pathological evaluation. Brain 138:2020–2033.
Wang C, et al. (2025) Cerebral perfusion correlates with amyloid deposition in patients with mild cognitive impairment due to Alzheimer's disease. J Prev Alzheimers Dis 12:100031.
Wechsler D (1987) *WMS-R: Wechsler Memory Scale–Revised : manual*. San Antonio: Psychological Corp. Harcourt Brace Jovanovich.
West KL, Zuppichini MD, Turner MP, Sivakolundu DK, Zhao Y, Abdelkarim D, Spence JS, Rypma B (2019) BOLD hemodynamic response function changes significantly with healthy aging. Neuroimage 188:198–207.
Zetterberg H, Bendlin BB (2021) Biomarkers for Alzheimer's disease—preparing for a new era of disease-modifying therapies. Mol Psychiatry 26: 296–308.
Zigmond MJ, Abercrombie ED, Berger TW, Grace AA, Stricker EM (1990) Compensations after lesions of central dopaminergic neurons: some clinical and basic implications. Trends Neurosci 13:290–296.